Arch. Metall. Mater. **67** (2022), 3, 837-842

DOI: https://doi.org/10.24425/amm.2022.139673

MUHAMMAD AQIB BUSHARAT[1], MUHAMMAD YASIN NAZ[1*],
SHAZIA SHUKRULLAH[1], MUHAMMAD ZAHID[2]

POST-SYNTHESIS MICROWAVE PLASMA TREATMENT EFFECT ON MAGNETIZATION AND MORPHOLOGY OF MANGANESE-IRON OXIDE NANOPARTICLES

The influence of microwave (MW) plasma on magnetization and morphology of sol-gel synthesized $MnFe_2O_4$ ferrite nanoparticles is investigated in this study. Manganese (II) nitrate hexahydrate, ferric (III) nitrate nanohydrate and citric acid were used to synthesize ferrite nanoparticles via a facile sol-gel route. These ferrite nanostructures were heat-treated at 700ºC and then given MW plasma treatment for 10 min. The pristine $MnFe_2O_4$ and plasma treated $MnFe_2O_4$ showed almost similar structural formation with a slight increase in crystallinity on plasma treatment. However, XRD peak intensity slightly increased after plasma treatment, reflecting better crystallinity of the nanostructures. The size of the particle increased from 35 nm to 39 nm on plasma treatment. It was challenging to deduce the surface morphology of the nanoparticles since both samples were composed of a mixture of big and small clusters. Clusters that had been treated with plasma were larger in size than pristine ones. The band gap energy of the pristine $MnFe_2O_4$ sample was about 5.92 eV, which increased to 6.01 eV after treatment with MW plasma. The saturation magnetization of $MnFe_2O_4$ sample was noted about 0.78 emu/g before plasma treatment and 0.68 emu/g after MW plasma treatment.

Keywords: Ferrite nanoparticles; microwave discharge; sol-gel synthesis; magnetic properties

1. Introduction

The ferrite nanoparticles are known for their large surface area to volume ratio and strong magnetization character. These nanoparticles are generally called transition metal oxides and have spinel structures. The magnetization of ferrite nanoparticles depends on the size, shape, surface morphology, and distribution of the crystallites [1-4]. Manganese ferrite nanoparticles show low magnetic losses and high permeability [5]. These nanoparticles find their applications in memory chips, magnetic recording devices, radiofrequency devices, antennas, microwave devices, transformer cores, telecommunication devices and electronics [6-9]. The synthesis of ferrites at lower temperatures saves energy and reduces the process cost. The possible synthesis methods include micro-emulsion, chemical co-precipitation, sol-gel, plasma-assisted CVD, hydrothermal techniques, etc [8]. The sol-gel technique has great potential for producing nanostructures of defined shapes and crystallinity. However, it leaves some oxides and unreacted gel in the final product. These impurities in the product may limit its applications. The majority of the spinel ferrites do not exhibit the properties generally needed for the fabrication of nanoscale devices for different applications. These materials show chemically inert nature and have low surface energies if they are not properly washed, calcined, and activated. The low surface energy restricts the functional groups from interacting with the material surface [9].

The nano-ferrite materials, synthesized through conventional methods, lack the key properties needed for their applications in major industries. Modifying the surface properties of ferrite nanoparticles after synthesis is an important way of making them clinically relevant materials. However, most conventional methods are energy-intensive and deteriorate the surface properties during treatment. Alternatively, plasmas discharges are also applied to generate the high energy reactive species for tailoring the specific surface properties and chemistry of such materials. In microwave plasma-driven synthesis of nanomaterials, the synthesis reaction is exposed to a low-pressure gas discharge under controlled conditions. Microwave plasma irradiation speeds up the synthesis reaction by increasing the molecular

[1] DEPARTMENT OF PHYSICS, UNIVERSITY OF AGRICULTUREFAISALABAD, 38040, PAKISTAN
[2] DEPARTMENT OF CHEMISTRY, UNIVERSITY OF AGRICULTURE FAISALABAD, 38040, PAKISTAN

* Corresponding Author E-mail: yasin603@yahoo.com

vibrations and decreasing the activation energy. The MW plasma oscillates the electrons in the discharge gas, which collide with neutral atoms or molecules and produce further electrons along with ions and other reactive species. When combined with MW plasma, the sol-gel method can alter the crystallinity, size and surface properties of the nanostructures [10-12].

The objective of this study was to synthesize $MnFe_2O_4$ nanoferrite by using a facile sol-gel route and to remove the impurities, dried gel and oxides from the sample by giving it low-pressure microwave plasma treatment. Manganese nitrate and ferric nitrate were used as starting materials for the synthesis of nano-ferrite. The as-synthesized ferrite nanoparticles were dried in an oven and calcined at 700ºC for 6 hours to induce good magnetic properties. The calcined product was treated with MW plasma of oxygen for 10 minutes in a low-pressure chamber. The pristine and MW plasma treated $MnFe_2O_4$ samples were analyzed for their morphology, magnetic response, particle size and chemical composition.

2. Materials and methods

2.1. Synthesis of ferrite nanoparticles

A simple sol-gel technique was used to produce manganese-iron oxide ferrite nanoparticles. Analytical grade ferric nitrate nanohydrate and manganese nitrate hexahydrate were taken as starting materials. The glassware was washed with deionized water before use to avoid contamination. To make a solution, Mn and Fe salts were mixed in a 1:2 ratio and dissolved in deionized water. The solution was stirred on a magnetic hot plate at 80ºC for 1 hour. Thereafter, citric acid was added dropwise to grow the sol from the mixture. On further heating, the sol changed to gel, which could settle down under continuous heating. The obtained material was heated in oven for 24 hours at 90ºC and ground into fine powder. The ground powder was dried again in an oven for 4 hours at 90ºC and then calcined at 700ºC for 6 hours to induce strong magnetic characteristics.

2.2. Plasma treatment of ferrite nanoparticles

The calcined $MnFe_2O_4$ ferrite samples were treated with MW plasma for 10 minutes in a low-pressure chamber. The low-pressure oxygen plasma is an economical practical and environmental friendly method of cleaning and etching metallic and nonmetallic materials. The oxygen plasma was produced in a vacuum-tight chamber by delivering power from a MW source of 1200 W capacity. The MW plasma was consisted of a microwave source, plasma chamber, shielding box, vacuum pump, thermocouples, vacuum gauge, sample holder, gas supply and microwave power controller. The MW plasma setup, used for the treatment of $MnFe_2O_4$ ferrite, is shown schematically in Fig. 1. The ferrite sample was taken in a boat and placed in the plasma chamber. The chamber was shielded, grounded and vacuumized with a rotary vacuum pump. The precursor gas was flushed into the chamber and the process pressure was maintained at 8 mbar throughout the treatment process. The microwave power was provided to the gas to break its molecules into atoms, electrons, ions, free radicals and electromagnetic radiations. The reactive species interacted with the sample and altered its physical, magnetic and structural properties.

The final product was characterized for particle size, surface morphology, magnetic field strength and structural changes. Scanning electron microscopy of the samples was performed to study the morphology of the ferrite nanoparticles before and after plasma treatment. Vibrating sample magnetometer was used to produce hysteresis lops to study magnetic properties. X-ray diffraction spectra were created to find out the particle and Miller indices of the product. A 550 Universal Interface, coupled with a magnetic field sensor, was employed to determine the magnetic field strength of the pristine and plasma-treated $MnFe_2O_4$.

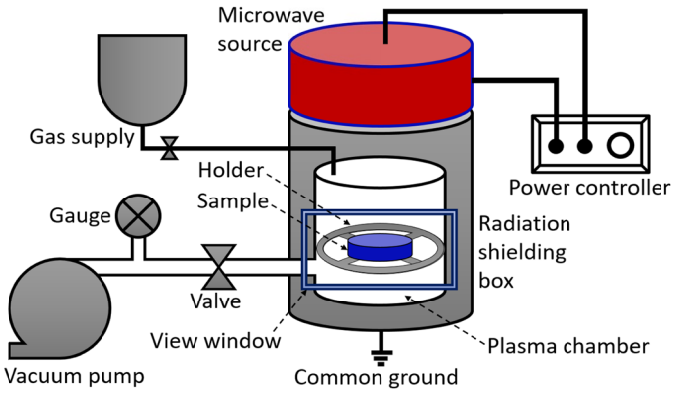

Fig. 1. A low-pressure MW plasma setup used for the modification of $MnFe_2O_4$ ferrite nanoparticles

3. Results and discussion

3.1. XRD analysis of ferrite nanoparticles

Nanomaterials have properties that vary from their bulk counterparts. These properties are of considerable importance for their applications in textile, medical, optical, electronic, defense, food, cosmetology, chemicals, catalyst and packing industries. Complete characterization of the nanomaterials is required for each application. In this study, the crystal structure, crystallinity and phases of conventionally calcined and microwave plasma treated ferrite nanoparticles were evaluated using XRD patterns. Fig. 2 shows XRD patterns of both untreated and plasma-treated $MnFe_2O_4$ samples. The diffraction peaks matched well the JCPDS card number 74-2403. The matched data confirmed the FCC structure of $MnFe_2O_4$ nanoparticles. XRD peaks of $MnFe_2O_4$ ferrite revealed (220), (311), (400), (422) and (511) planes in structure. Although both pristine and plasma-treated $MnFe_2O_4$ samples exhibited similar phases and planes, the peak intensity showed a slight increment after plasma treatment. An increase in peak intensity reflects an improvement in crystallinity of

the nanostructures. Scherrer's formula was employed to calculate the crystallite size of $MnFe_2O_4$ nanoparticles.

$$L = \frac{0.89\lambda}{\beta \cos\theta} \quad (1)$$

Where, θ is Bragg angle, L is the grain size, λ is the wavelength of X-rays and β is the full width at half maxima. The plasma produced some oxidative species like O_3, H_2O_2, HO_2^-, and OH^-, which interacted with the ferrite nanoparticles. The particle size increased after plasma treatment due to oxidation and then the aggregation of the nanoparticles. The particle size of pristine $MnFe_2O_4$ sample was around 35 nm, which grew to 39 nm after 10 minutes of MW plasma exposure. The lattice constant of the untreated and MW plasma-treated $MnFe_2O_4$ samples was measured at about 8.3544 Å and 8.4885 Å, respectively. TABLE 1 shows that the lattice constant and crystallite volume slightly increased on plasma treatment.

TABLE 1

The particle size, lattice constant and volume of the ferrite nanoparticles

Sample	Crystallite size (nm)	Lattice constant (Å)	Volume (A^3)
Untreated	35	8.3544	571.66
Plasma treated	39	8.4885	613.11

Jacob et al. [13] synthesized nickel ferrite nanoparticles using both sole-gel and co-precipitation techniques. They investigated the magnetic and morphological properties of the $MnFe_2O_4$ nanoparticles using different intrusive and non-intrusive techniques. The sole-gel technique produced more crystalline nanoparticles as compared to the co-precipitation technique. Particles were spherical in shape and exhibited narrow size distribution. The nanoparticles, synthesized via co-precipitation technique, exhibited unpredictable shapes, wide size distribution and small sizes. Sankaranarayanan et al. [14] synthesized ferrite nanoparticles by sol-gel and co-precipitation strategies at different temperatures. The sole-get technique produced nanoparticles of improved permittivity and structural properties. Kesavamoorthi et al. [15] produced ferrite nanoparticles by sol-gel strategy. They calcined the particles at 600°C for 2 hours. XRD analysis revealed octahedral and tetrahedral shapes of the metal oxide nanoparticles. Venkatesh et al. [8] synthesized the ferrite nanoplatelets using the microwave-driven combustion method. Trisodium citrate was used as a precursor. The synthesized samples were identified as phase-pure ferrite nanoplatelets with average particle sizes in the range of 40-50 nm. The samples exhibited a soft ferromagnetic nature with high saturation magnetization. Isfahani, et al. [16] synthesized ferrite nanoparticles by a delicate mechanochemical route technique. The nano-ferrites synthesized via the mechanochemical route were composed of nanocrystalline structures with an average crystallite size of around 30 nm to 40 nm. The crystallite size in the presented work agrees well with the published literature.

3.2. SEM analysis of ferrite nanoparticles

The surface morphology of pristine and plasma-modified manganese ferrite nanoparticles was studied from SEM micrographs. SEM illustration of both samples is provided in Fig. 3. It was difficult to define the morphology since samples were formed of a mixture of clearly differentiable small and large clusters. All clusters exhibited undefined geometry. In plasma-treated $MnFe_2O_4$, the larger clusters were small in number than the pristine $MnFe_2O_4$. However, the size of treated $MnFe_2O_4$ clusters was significantly larger than the pristine $MnFe_2O_4$ clusters. An increase in cluster size of plasma-treated $MnFe_2O_4$ might be due to the aggregation of smaller clusters into larger clusters during treatment. The microwave plasma treatment raised the sample temperature upto 300ºC. The morphology and structure of nanoparticles changed slightly due to their oxidation under a combined effect of heating and plasma reactive species. The plasma exposure also cleared the sample from the burnt gel, carbon and other unwanted products. The $MnFe_2O_4$ particles recrystallized without undergoing major phase changes due to the weakening of the surface bonds during plasma exposure.

Also, the plasma treated clusters exhibited a porous surface. The porous areas are highlighted in circles in Fig. 3. The SEM images of pristine and MW plasma treated $MnFe_2O_4$ samples

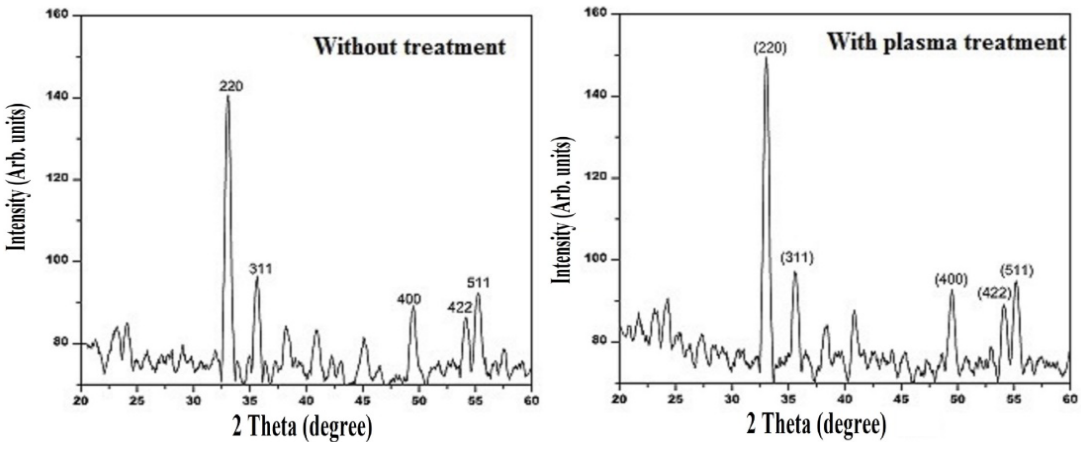

Fig. 2. XRD spectra of pristine and MW plasma-treated $MnFe_2O_4$ nanoparticles

are showin in Figs 3(a) and 3(b), respectively. These plasma species transferred the energy to surface atoms. These surface atoms excite and leave the surface due to the occurrence of the sputtering phenomenon during plasma exposure. The pore size may increase with an increase in plasma input energy. More energetic plasma species mean great damage at the surface will happen. Another reason for the appearance of pores on the surface is the removal of impurities from the sample. It was also observed in XRD patterns where peak intensity was slightly increased after plasma treatment. Frolova and Derhachov [17] reported agglomerated of nanoparticles exposed to plasma due to magnetic dipole interaction between the nanoparticles. The head produced during plasma-sample interaction may also have caused agglomeration. Agglomeration on heating is a typical characteristic of spinel ferrites [18]. Plasma treatment is also a type of low-temperature calcination, which becomes more effective under the interaction of plasma species with the sample.

3.3. UV-visible analysis

UV-visible analysis provides insight into the optical properties of the materials. It also provides information about sub-band gap defect states, especially for nanostructures of ferrites. Fig. 4 shows UV-visible spectra of pristine and MW plasma-

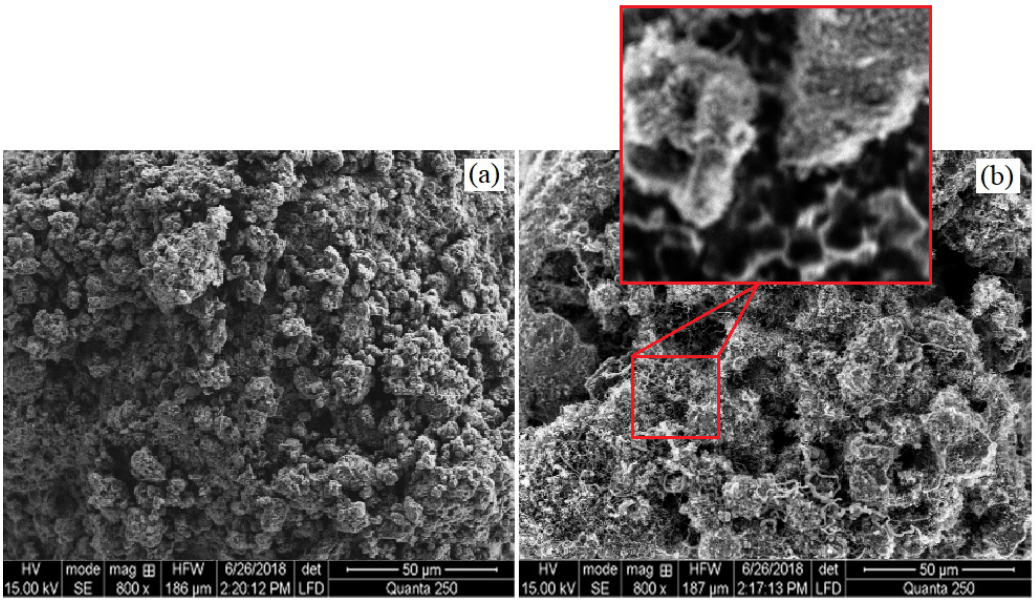

Fig. 3. SEM illustration of (a) pristine and (b) MW plasma treated $MnFe_2O_4$ nanoparticles

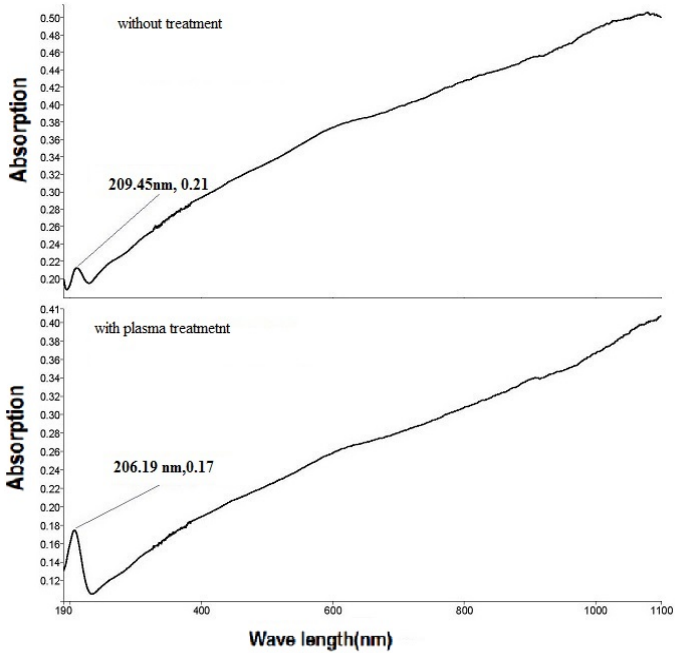

Fig. 4. UV-visible pattern of pristine and MW plasma treated $MnFe_2O_4$ nanoparticles

treated $MnFe_2O_4$ nanoparticles. An absorption peak of pristine $MnFe_2O_4$ ferrite sample was found around 209 nm. The MW plasma-treated $MnFe_2O_4$ sample showed an adsorption peak around 206 nm. These absorption peaks revealed low absorbance by the tested ferrite samples in the visible and infrared regions of the solar spectrum. The adsorption peak of the plasma treated sample appeared 3 points earlier on horizontal axis, which might be due to plasma heating during treatment. The band gap energy of the pristine $MnFe_2O_4$ sample was about 5.92 eV, which increased to 6.01 eV after MW plasma treatment. Generally, band gap energy declines with a rise in particle size. In this case, both band gap energy and particle size were increased slightly after plasma treatment. A larger band gap indicates that more energy would be required to excite the electrons to the conduction band from the valance band of an atom.

3.4. Magnetic properties of ferrite nanoparticles

Magnetic properties of pristine and MW plasma-treated $MnFe_2O_4$ samples were accessed by generating their hysteresis

loops. Fig. 5 shows the hysteresis loops, where both pristine and MW plasma treated samples showed ferromagnetic behavior. The observed hysteresis loops reflect the formation of nanoparticles of $MnFe_2O_4$ ferrite. The crystallize size increased after treating the samples with MW plasma. The magnetic domain size grows in lockstep with the crystallite size. The growing atomic spins, aligned with the applied magnetic field, created strong magnetization [19]. Since plasma treatment is a type of low-temperature calcination, it becomes more effective during contact of plasma species with $MnFe_2O_4$ sample. As revealed earlier, the particle size was slightly increased on plasma treatment. In response, the magnetization of the sample was also increased. At lower temperatures, different factors may affect the magnetic properties of the spinel ferrites. These factors are the presence of dead layers in sample, size confinements, spin transitions and thermal dependence of magnetic properties [19-21].

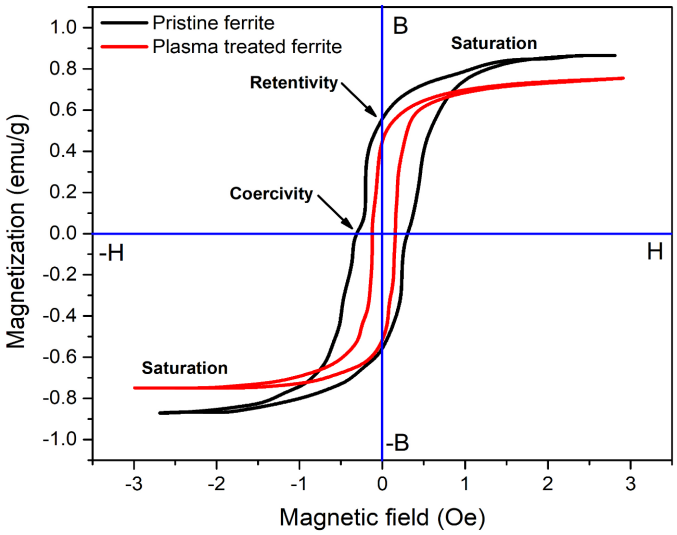

Fig. 5. VSM profiles of pristine and MW plasma-treated $MnFe_2O_4$ nanoparticles

TABLE 2 shows coercivity and saturation magnetization measured from the hysteresis loops. The pristine $MnFe_2O_4$ ferrite sample exhibited relatively higher saturation magnetization as compared to MW plasma-treated $MnFe_2O_4$ sample. The small saturation magnetization of MW plasma-treated sample shows well-ordered parameter behavior of ferromagnet materials [20]. The saturation magnetization of pristine and MW plasma-treated $MnFe_2O_4$ was about 0.78 and 0.68 emu/g, respectively. The coercivity of MW plasma-treated $MnFe_2O_4$ also exhibited a decreasing trend. The coercivity of pristine $MnFe_2O_4$ was about 0.3 kOe, which decreased to 0.1 kOe after MW plasma treatment.

TABLE 2

Magnetic parameters of pristine and MW plasma treated $MnFe_2O_4$ nanoparticles

Sample	M_s (emu/g)	M_r (emu/g)	$R_s = M_r/M_s$	H (kOe)
Before Treatment	0.78	0.5	0.64	0.3
After Treatment	0.68	0.4	0.58	0.1

The magnetic field strength of $MnFe_2O_4$ nanoparticles is reported in Fig. 6. The magnetic field strength was measured using a 550 Universal Interface coupled with a magnetic field sensor. It is a quantitative method of measuring the weakness or strength of the magnetic field of a magnet. The magnetic field strength increased after plasma treatment of ferrite nanoparticles. The amount of atomic spins, aligned with the applied magnetic field, increased with plasma treatment. In response, the ferrite sample exhibited a high magnetic field strength. The field strength did not depend over time and showed consistent behavior with the passage of time. Since magnetic field strength measurements were made in an open atmosphere, some downward spikes appeared in the plots. These spikes might be due to interference of dust particles or vibrations experienced by the sensor during measurements [21].

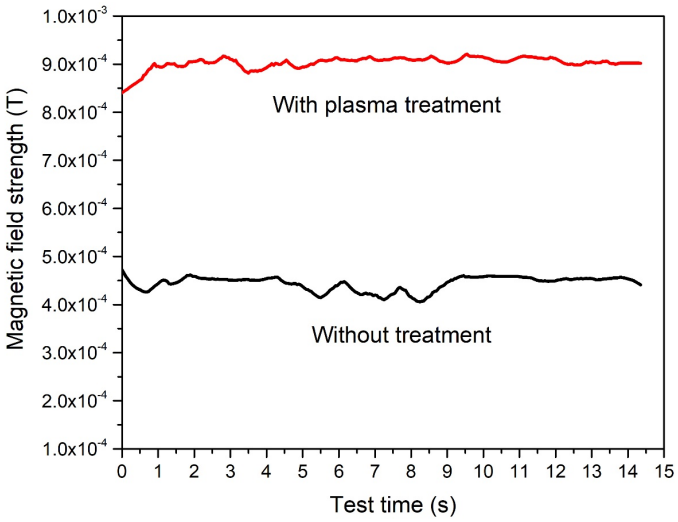

Fig. 6. Magnetic field strength of untreated and MW plasma treated ferrite nanoparticles

4. Conclusions

Manganese $MnFe_2O_4$ ferrites were synthesized by following a facile sol-gel route. Post-synthesis microwave plasma treatment was given to these ferrite nanoparticles. Although both pristine and MW plasma-treated $MnFe_2O_4$ samples exhibited similar phases and planes, XRD peak intensities of plasma-treated $MnFe_2O_4$ were slightly higher when compared with pristine $MnFe_2O_4$ sample. The particle size was increased after plasma treatment due to oxidation followed by agglomeration of the nanoparticles. The pristine $MnFe_2O_4$ samples have an average particle size of 35 nm, which grew to 39 nm after 10 minutes of plasma treatment. The lattice parameter of pristine and MW plasma-treated $MnFe_2O_4$ samples was about 8.3544 Å and 8.4885 Å, respectively. The shape of the nanoparticles was difficult to determine since both pristine and plasma-treated samples contained big clusters intermingled with smaller clusters. The band gap energy of pristine $MnFe_2O_4$ was about 5.92 eV, which increased to 6.01 eV after MW plasma exposure. The saturation magnetization of the pristine $MnFe_2O_4$ sample was 0.78 emu/g,

which was reduced to 0.68 emu/g on MW plasma treatment. Similarly, coercivity decreased from 0.3 kOe to 0.1 kOe after MW plasma therapy of $MnFe_2O_4$ nanoferrite.

Conflicts of Interest

There is no conflict of interest for publishing this paper.

REFERENCES

[1] A. Nairan, M. Khan, U. Khan, M. Iqbal, S. Riaz, S. Naseem, Temperature dependent magnetic response of antiferromagnetic doping in cobalt ferrite nanostructures, Nanomaterials **6** (4), 73 (2016). DOI: https://doi.org/10.3390/nano6040073

[2] Y. Khan, S. Shukrullah, M. Y. Naz, A. Ghaffar, I. Ahmad, S. Alsuhaibani, Ferrocene Weight Optimization for CVD Growth of Carbon Nanotubes Over $Si/SiO_2/Al_2O_3$, Digest Journal of Nanomaterials and Biostructures **12** (4), 957-963, (2017).

[3] M.A. Munir, M.Y. Naz, S. Shukrullah, M.T. Ansar, G. Abbas, M.M. Makhlouf, Microwave plasma treatment of NiCuZn ferrite nanoparticles: A novel approach of improving opto-physical and magnetic properties, Appl. Phys. A. **128** (4), 1-10, (2022). DOI: https://doi.org/10.1007/s00339-022-05480-6

[4] I. Toqeer, M.Y. Naz, Y. Khan, M. Azam, R. Meer, Morphological and magnetic response of copper-substituted nickel ferrite nanoparticles, Philosophical Magazine Letters **99** (2), 67-76, (2019).

[5] S. Yang, J.G. Kim, Magnetic Properties of $(Nia\text{-}Znb)_XCu_{1-X}$ Ferrite Nanoparticle Fabricated by Sol-Gel Process, Arch. Metall. Mater. **62** (2), 197-1200 (2017).
DOI: https://doi.org/10.1515/amm-2017-0176

[6] M.J. Akhtar, M. Younas, Structural and transport properties of nanocrystalline $MnFe_2O_4$ synthesized by co-precipitation method, Solid State Sci. **14** (10), 1536-1542 (2012).
DOI: https://doi.org/10.1016/j.solidstatesciences.2012.08.026

[7] A. Alarifi, N.M. Deraz, S. Shaban, Structural, morphological and magnetic properties of $NiFe_2O_4$ nano-particles, J. Alloys Compd. **486**, 501-506 (2009).
DOI: https://doi.org/10.1016/j.jallcom.2009.06.192

[8] M. Venkatesh, G.S. Kumar, S. Viji, S. Karthi, E.K. Girija, Microwave assisted combustion synthesis and characterization of nickel ferrite nanoplatelets, Mod. Electron. Mater. **2** (3), 74-78 (2016).
DOI: https://doi.org/10.1016/j.moem.2016.10.003

[9] M.G. Naseri, E.B. Saion, H.A. Ahangar, M. Hashim, A.H. Shaari, Simple preparation and characterization of nickel ferrite nanocrystals by a thermal treatment method, Powder Technol. **212** (1), 80-88 (2011).
DOI: https://doi.org/10.1016/j.powtec.2011.04.033

[10] J.L.H. Chau, C.C. Yang, Surface modification of silica nanopowders in microwave plasma, J. Exp. Nanosci. **9** (4), 357-361 (2014).
DOI: https://doi.org/10.1080/17458080.2012.661473

[11] L. Dreesen, F. Cecchet, S. Lucas, DC magnetron sputtering deposition of titanium oxide nanoparticles: Influence of temperature, pressure and deposition time on the deposited layer morphology, the wetting and optical surface properties, Plasma Processes Polym. **6**, S849-S854 (2009).
DOI: https://doi.org/10.1002/ppap.200932201

[12] S. Shukrullah, M.Y. Naz, N.U.H. Altaf, A. Ali, Effect of DC voltage on morphology and size distribution of silver nanorods synthesized through plasma-liquid interaction method, Mater. Today: Proc. (2020). DOI: https://doi.org/10.1016/j.matpr.2020.04.683

[13] B.P. Jacob, A. Kumar, R.P. Pant, S. Singh, E.M. Mohammed, Influence of preparation method on structural and magnetic properties of nickel ferrite nanoparticles, Bull. Mater. Sci. **34** (7), 1345-1350 (2011). DOI: https://doi.org/10.1007/s12034-011-0326-7

[14] V.K. Sankaranarayanan, C. Sreekumar, Precursor synthesis and microwave processing of nickel ferrite nanoparticles, Curr. Appl. Phys. **3** (2), 205-208 (2003).
DOI: https://doi.org/10.1016/S1567-1739(02)00202-X

[15] R. Kesavamoorthi, A.N. Vigneshwaran, V. Sanyal, C.R. Raja, Synthesis and characterization of nickel ferrite nanoparticles by sol-gel auto combustion method, J. Curr. Chem. Pharm. Sci. **9** (1), 1-3 (2016).

[16] M.J.N. Isfahani, M.J. Fesharaki, V. Šepelák, Magnetic behavior of nickel-bismuth ferrite synthesized by a combined sol-gel/thermal method, Ceram. Int. **39** (2), 1163-1167 (2013).
DOI: https://doi.org/10.1016/j.ceramint.2012.07.040

[17] L. Frolova, M.P. Derhachov, The Effect of Contact Non-equilibrium Plasma on Structural and Magnetic Properties of $MnXFe_3$-XO_4 Spinels, Nanoscale Res. Lett. **12**, 505 (2017).
DOI: https://doi.org/10.1186/s11671-017-2268-5

[18] M. Singh, S.P. Sud, Controlling the properties of magnesium-manganese ferrites, J. Mater. Sci. Eng. B **83** (1), 180-184 (2001).
DOI: https://doi.org/10.1016/S0921-5107(01)00514-1

[19] M. Stoia, E. Muntean, C. Păcurariu, C. Mihali, Thermal behavior of $MnFe_2O_4$ and $MnFe_2O_4$/C nanocomposite synthesized by a solvothermal method, Thermochim. Acta **652**, 1-8 (2017).
DOI: https://doi.org/10.1016/j.tca.2017.03.009

[20] M.Y. Naz, M. Irfan, S. Shukrullah, I. Ahmad, A. Ghaffar, U.M. Niazi, S. Rahman, M. Jalalah, M.A. Alsaiari, M.K.A. Khan, Effect of microwave plasma treatment on magnetic and photocatalytic response of manganese ferrite nanoparticles for wastewater treatment, Main Group Chem. **20** (3), 423-435, (2021).
DOI: https://doi.org/10.3233/MGC-210065

[21] A. Thakur, M. Singh, Preparation and characterization of nanosize Mn0.4Zn0.6 Fe2O4 ferrite by citrate precursor method, Ceram. Int. **29** (5), 505-511 (2003).
DOI: https://doi.org/10.1016/S0272-8842(02)00194-3